Light-Driven Reversible Transformation between Self-Organized Simple Cubic Lattice and Helical Superstructure Enabled by a Molecular Switch Functionalized Nanocage

Kang Zhou, Hari Krishna Bisoyi, Jian-Qiu Jin, Cong-Long Yuan, Zhen Liu, Dong Shen, Yan-Qing Lu, Zhi-Gang Zheng,* Weian Zhang,* and Quan Li*

Self-organized stimuli-responsive smart materials with adjustable attributes are highly desirable for a plethora of device applications. Simple cubic lattice is quite uncommon in soft condensed matter due to its lower packing factor. Achieving a stable simple cubic soft lattice and endowing such a lattice with dynamic reconstruction capability solely by a facile light irradiation are of paramount significance for both fundamental studies and engineering explorations. Herein, an elegant stable self-organized simple cubic soft lattice, i.e., blue phase II, in a chiral liquid crystal (LC) system is disclosed, which is stable down to room temperature and exhibits both reversible lattice deformation and transformation to a helical superstructure, i.e., cholesteric LC, by light stimulation. Such an amazing trait is attained by doping a judiciously designed achiral photoresponsive molecular switch functionalized polyhedral oligomeric silsesquioxane nanocage into a chiral LC host. An unprecedented reversible collapse and reconstruction of such a high symmetric simple cubic blue phase II driven by light has been achieved. Furthermore, a well-defined conglomerate micropattern composed of simple cubic soft lattice and helical superstructure, which is challenging to fabricate in organic and inorganic crystalline materials, is produced using photomasking technology. Moreover, the promising photonic application based on such a micropattern is demonstrated.

Variety of exotic three dimensional (3D) lattice structures, such as the face-centered and body-centered cubic (bcc) colloidal crystals,[1] the "open" lattice (i.e., Kagome lattice) constructed by the Janus colloidal sphere with two attractive patches centered on two poles,[2] the triclinic lattice in an inorganic nanoparticle loaded nematic colloid,[3] and the topological structures formed by liquid crystal (LC) colloid,[4] have been developed in the past decade that elaborate the diversity of soft superstructure. In general, the face-centered cubic (fcc) is the most common Bravais lattice in soft condensed crystals in accordance with the close-packed principle;[5] however, configuring a stable soft simple cubic (sc) lattice is still a formidable and challenging task due to the lower packing factor, which remarkably increases the free energy and reduces the stability of the lattice structure. Moreover, stimuli-driven, facile and reversible transformation of soft simple cubic lattice to other self-organized functional 3D and one dimensional (1D) superstructures remains a formidable undertaking. Manipulating, deforming, and reconstructing the structure and function of 3D self-organized soft superstructures using external stimuli is a booming theme and is of both scientific and technological significance in the framework of bottom-up mesoscopic and molecular engineering; however, obtaining such attributes has been demanding.

K. Zhou, C.-L. Yuan, Z. Liu, Prof. D. Shen, Prof. Z.-G. Zheng
Department of Physics
East China University of Science and Technology
Shanghai 200237, China
E-mail: zgzheng@ecust.edu.cn
Dr. H. K. Bisoyi, Prof. Q. Li
Liquid Crystal Institute and Chemical Physics Interdisciplinary Program
Kent State University
Kent, OH 44242, USA
E-mail: qli1@kent.edu

J.-Q. Jin, Prof. W. Zhang
Shanghai Key Laboratory of Functional Materials Chemistry
East China University of Science and Technology
Shanghai 200237, China
E-mail: wazhang@ecust.edu.cn
Prof. Y.-Q. Lu
National Laboratory of Solid State Microstructures
Collaborative Innovation Center of Advanced Microstructures
and Colleague of Engineering and Applied Sciences
Nanjing University
Nanjing 210093, China

The ORCID identification number(s) for the author(s) of this article can be found under https://doi.org/10.1002/adma.201800237.

**ADVANCED
SCIENCE NEWS**
www.advancedsciencenews.com

**ADVANCED
MATERIALS**
www.advmat.de

Blue phase (BP), a specific LC phase in which molecules arrange in double twisted cylinders (DTCs), commonly exists between the isotropic phase and cholesteric (N*) phase in systems possessing high chirality. Such DTCs are topologically stacked as the bcc lattice, i.e., BPI, or the sc lattice, i.e., BPII, by molecular self-organization under appropriate circumstances. The randomly aligned LC molecules are filled into the interspaces between two adjacent DTCs as the defects to reduce free energy of the system, forming a typical frustrated phase. Lattice constants of the soft cubic BPs (BPI and BPII) are determined by the helical pitch of the chiral LC, which are comparable with the wavelength of visible light, thus qualifying them as soft photonic crystals.[6] In contrast to the bcc lattice of BPI, the sc lattice of BPII is more desirable on account of its better stimuli-responsiveness, manipulation compliance, and a more satisfying photonic performance in applications.[7] However, not all high chirality cholesteric LC (CLC) systems exhibit such soft sc lattice, and even if some do, the structure of lattice is rather unstable owing to the low packing factor of sc stacking as aforementioned. As a consequence, the fabrication of a stable LC sc lattice, i.e., BPII, is still an inevitable scientific issue attracting accumulated attentions. Furthermore, the readily structural manipulation, deformation and reversible reconstruction of such BPII sc lattice via external stimuli are considered to be crucial and profound for promoting and broadening its application potential. Although the tunability of lattice constant of BPI bcc[8] and the transformation between BPII sc and BPI bcc through light irradiation have been realized,[9] and in addition, the fcc and bcc colloidal crystal templated by BP defects has also been created recently,[10] the reversible transformation of stable BPII sc lattice to a 1D helical superstructure by facile light irradiation is still intractable and remains an unexplored avenue with potential opportunities.

Recently, vertical alignment of nematic LC on the surface covered with polyhedral oligomeric silsesquioxane (POSS) due to the lower tension at the interface between LC and POSS was found[11] and the relevant photonic applications based on such fantastic attribute were developed.[12] Moreover, inspired by the prior investigations, a slight widening of BP temperature range for less than 2 °C by mixing a small amount of pure POSS[13] and a reduction of driving voltage of a polymer-stabilized BPLC containing POSS segments in polymer network[14] have been realized. These previous works have confirmed the advantages of POSS on the stabilization of cubic BP, and the challenges of making it compatible with the host LC have been indicated. On the other hand, structural manipulations of BP lattice by light were achieved in a BPLC system mixed with photoresponsive molecular switches or motors,[8a,9,15] gold nanorods,[16] and the polyoxometalate organic–inorganic hybrids.[17] Besides, a stable BPII has been realized by polymer stabilization, which is not photoresponsive.[18] However, deformation of a BPII sc lattice leading to reversible transformation to N* phase using light irradiation has never been found and reported to date. Herein, we demonstrate wide-range stabilization of self-organized BPII soft sc lattice by doping a judiciously designed photoresponsive molecular switch functionalized POSS nanocage and its reversible transformation

to the helical superstructure of CLC solely driven by light irradiation. The mesogenic photoresponsive moieties grafted on POSS possessing a rod-like geometry, which is similar to the molecular structure of LC used herein and thus we have reason to believe high compatibility and an improved solubility of such functionalized POSS in the BP host. To the best of our knowledge, this work first endows a stable soft sc lattice with both the structural deformation and reconstruction by light, which simultaneously shines a broad way for stimuli-responsive soft crystals for application in crystallography and photonics, and could inspire the new scientific and technical ideas and insights into other relevant fields.

The molecular switch functionalized nanocage was synthesized by grafting photosensitive azobenzene moieties on eight vertices of the POSS through thiol-ene click reaction and is denoted as Azo-POSS (**Figure 1**a). The synthesis of this organic/inorganic hybrid compound has been described and characterized through spectroscopic and analytical techniques (see Supporting Information). Moreover, the photoresponsiveness of Azo-POSS was investigated by recording the change in its absorption spectra during a UV light irradiation with the intensity of 3.0 mW cm^{-2} (Figure S2a, Supporting Information). A BPLC host was prepared by homogeneously mixing a common nematic LC, TEB3X and chiral agent, R5011, which possesses BPII phase with a soft sc lattice structure in a narrow temperature range of ≈1.6 °C, i.e., from 57.0 to 55.4 °C, determined from the continuous blue-shift of the reflection spectrum (Figure S1, Supporting Information) during the cooling in accordance with previous reports.[6b,7a,19] Different quantities of the photosensitive Azo-POSS were blended with the BPLC host to enable photoresponsiveness of the mixtures. When the content of Azo-POSS was 2.0 wt%, the sample showed a typical BP texture displaying a colorful platelet and a conspicuous blue-shift of the corresponding reflection spectrum upon cooling from 55.6 to 51.4 °C (Figure S3, Supporting Information), which indicated the occurrence of BPII in the system. Moreover, the Kössel diagram, corresponding to a bluish green texture at 52.0 °C (Figure 1b-I), presented a circular ring pattern (Figure 1c-I), which was almost invariable in the whole cooling process, further corroborating the sc lattice of BPII. Here, an interesting and noteworthy aspect is the conspicuous stabilization of sc lattice of BPII after doping the Azo-POSS, i.e., a widening of BPII temperature range from 1.6 to 4.2 °C, indicating a significant difference with other photoresponsive systems used previously.

Photoresponsiveness of such BPII sc soft lattice, a pivotal aspect, was performed by a continual irradiation with a 365 nm UV light-emitting diode (LED) with an output light intensity of 1.0 mW cm^{-2} at a temperature close to the lower end of BPII range, i.e., 52.0 °C. BPII lattice exhibited an obvious change in reflection color, from the original bluish green, passing through bright green, yellow and orange, to the red with a duration of exposure for 24 s (Figure 1b-I–V), accompanied by a continuous red-shift of the reflection spectrum from 508 to 610 nm (Figure S4, Supporting Information). Further irradiation did not shift the reflection wavelength of the BPII;[8b,17] however, it resulted in a phase transition to the chiral nematic (N*) phase, i.e., cholesteric phase, starting at 28 s (Figure 1b-VI) and the N*
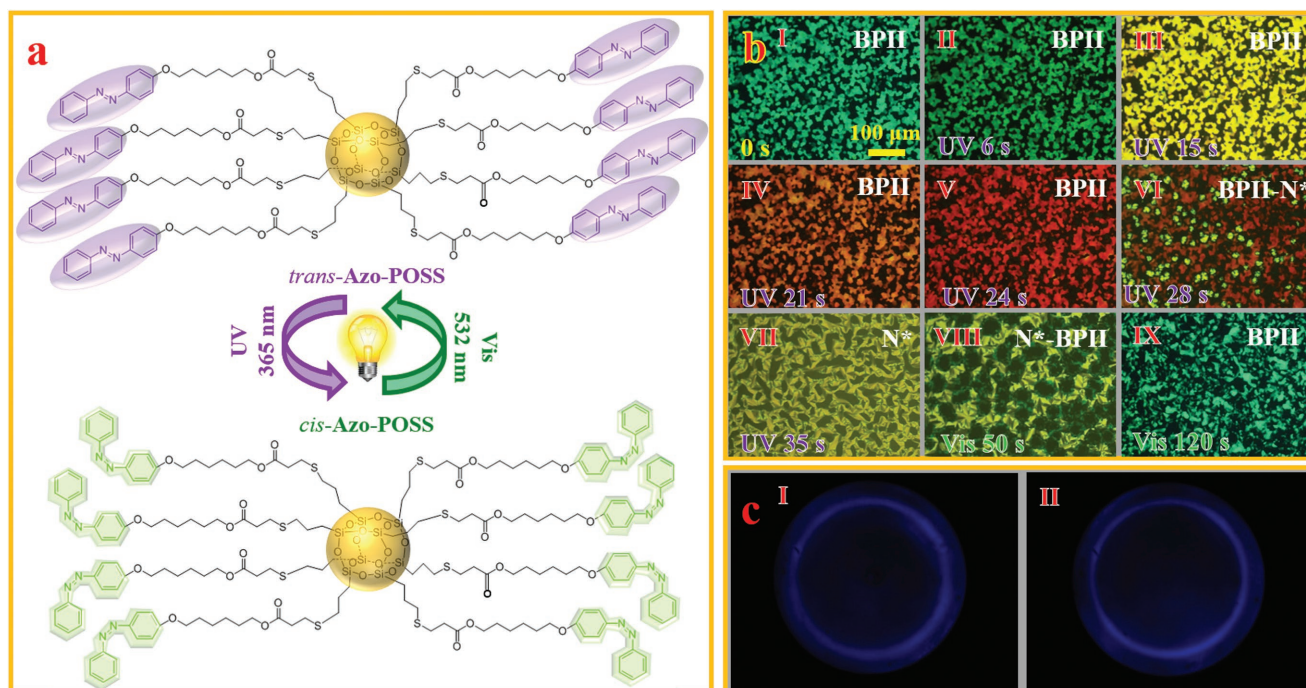
Figure 1. Light-driven reversible transformation between self-organized BPII soft sc lattice and a helical superstructure. a) Schematically depicted the photoisomerization of Azo-POSS from the *trans*-conformation to the *cis*-conformation by the irradiation of 365 nm UV light; a following irradiation with 532 nm visible light recovers such *cis*-conformation to *trans*-conformation. b) The deformation of self-organized BPII sc lattice during UV irradiation, showing the changes of reflection color from the original (I) bluish green, passing through (II) the green (6 s duration), (III) yellow (15 s duration), (IV) orange (21 s duration), to (V) the red (24 s duration). A further UV irradiation led to (VI, VII) the transition from such sc BPII to N*; (VIII, IX) the N* structure gradually reconstructed to BPII sc lattice with a following irradiation of 532 nm laser for about 120 s. Herein, the concentration of Azo-POSS was controlled at 2.0 wt%. The output light intensities of UV and laser were 1.0 and 10.0 mW cm^{-2}, respectively. Scale bar: 100 μm. c) Kössel diagrams at (I) the original state, i.e., corresponding to the texture shown in (b-I,II) the reconstructed BPII sc lattices, i.e., corresponding to the texture shown in (b-IX), respectively, displayed a similar circular ring pattern.

phase fully developed in 35 s of UV irradiation (Figure 1b-VII). The N* phase was incapable of recovering back to BP even after keeping the sample in dark for more than 48 h, probably owing to less defect of N* phase. However, upon visible light irradiation with a 532 nm laser (10.0 mW cm^{-2}) for 50 s, it was noticed that the low symmetric N* phase began to recover to the high symmetric BPII sc arrangement (Figure 1b-VIII). The BPII was fully developed in 120 s of irradiation with visible light (Figure 1b-IX). This recovered BPII exhibited similar optical texture and temperature range to those of the original BPII as confirmed by the observation of typical circular ring Kössel diagram (Figure 1c-II) and the blue-shift behavior of the reflection spectrum during cooling process (Figure S5, Supporting Information). Such reversible transformation between BPII and N* phase using alternate irradiation of UV and visible light can be repeated at least 30 times without any changes on such light switching, which is unprecedented though the transitions of BPII-BPI and BPI-N* have been reported recently. The specific dynamic phase switching between the sc and the helical superstructure resulted mainly from the photoisomerization of the molecular switch functionalized nanocage, Azo-POSS. The overall geometry and size of Azo-POSS reversibly changes during light irradiation owing to the conversion between the elongated *trans*-isomers and the bent *cis*-isomers of the azobenzene moieties grafted onto the vertices of POSS, which inevitably influences the arrangement of surrounding LC molecules,

and spread to the whole sample due to the "soft" property of LC materials, and thereby further results in the structural deformation of cubic BPII, including the elongation of lattice constant as well as the transformation between BPII and N*. Such lattice deformation was probably caused by the reduction of overall chirality of the system, thus leading to the aforementioned red-shift of the reflection spectrum (Figure S4, Supporting Information) and the collapse of the BPII sc lattice during UV irradiation.[20] The photoinduced transition between BPII and N* phase was also achieved at 55.0 °C close to the upper end of the BP range (Figure S6a, b, Supporting Information) in the mixture, which indicates that the reversible light-driven process can be effectively executed in the whole BPII range. Such observations revealed the first achievement of dynamic and reversible deformation and reconstruction of a sc soft lattice solely by facile light irradiation.

Inspired by the significant extension of BPII range after mixing a small amount of photosensitive Azo-POSS, and encouraged by the observation of the fantastic and reversible light-driven switching between BPII sc soft lattice and N* helical superstructure, we set out to increase the content of Azo-POSS in the BPLC host. As expected, temperature range of BPII extended gradually with increase in the amount of the photosensitive additive (Table S1, Supporting Information) due to the weakening on interfacial tension between defects and DTCs induced by Azo-POSS, which reduces the interfacial
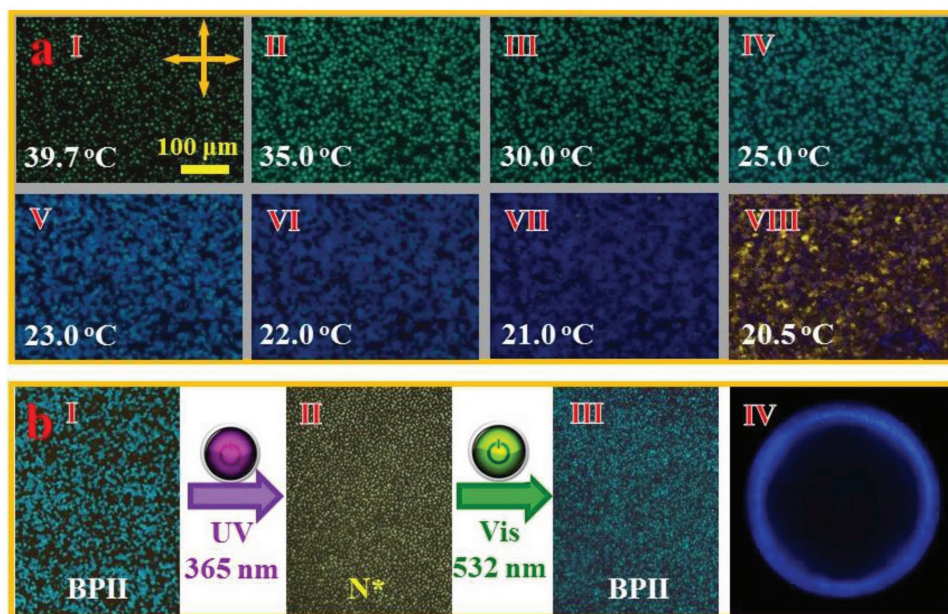
**ADVANCED
SCIENCE NEWS**
www.advancedsciencenews.com

**ADVANCED
MATERIALS**
www.advmat.de

Figure 2. Light-driven dynamic stable BPII sc lattice. a) The BPII texture, appearing at the temperature of (I) 39.7 °C, was maintained until the sample was cooled to (VIII) a temperature lower than 20.7 °C, i.e., the transition temperature from sc BPII to N*. The concentration of Azo-POSS was 26.0 wt%. b) Light-driven reversible transformation between BPII sc lattice and 1D helical N* phase was performed at room temperature, i.e., 25.0 °C. The original (I) sc BPII transited to (II) N* after a UV irradiation for 5 s, while N* was recovered to (III) BPII by stimulation with a 532 nm laser for 12 s, presenting a similar (IV) circular ring Kössel diagram. Light intensities of UV and visible light lasers used herein were 1.0 and 10.0 mW cm⁻², respectively. Scale bar: 100 µm.

energy on one hand, and the specific nanostructure of Azo-POSS, which decreases the excess free energy[21] on the other hand. Though the temperature range of the BP II was widened, both isotropic to BPII ($T_{\text{Iso-BPII}}$) and the BPII to N* ($T_{\text{BPII-N*}}$) reduced in the mixtures. Surprisingly, a stable BPII with a wider temperature range from 39.7 to 20.7 °C (**Figure 2**a, Table S1, Supporting Information), covering the typical room temperature (i.e., 25.0 °C), was obtained as the content of Azo-POSS reached 26.0 wt%. The reflection spectrum of the BPII shows a continuous blue-shift of the peak (Figure S7a, Supporting Information) in the whole cooling process. It is worth noting here that the observed temperature range of 19 °C is the widest with respect to a photoresponsive BPII sc lattice by molecular additives so far. The BPII range was further confirmed by the normalized capacitance (i.e., C_T/C_0, in which C_T represents the capacitance at a certain temperature, T, lower than the clearing point of the sample, while C_0 is the capacitance at the isotropic state) of the material during cooling process, which was in accordance with the fact that LC capacitance is sensitive to change in director field organization (Figure S7b, Supporting Information)[22] and was accurate for reflecting a real phase transition behavior of the sample confined in a micron-scaled-thick cell with the significant interfacial effects on the arrangement of LC molecules.[23] Such normalizations exhibited an initial decrease, passing through a plateau with a slight decrease in the range from 39.6 to 20.8 °C, and followed by an abrupt descending due to the weakening of orientated isotropy of LC molecules, thereby leading to the decrease of average permittivity of the system. Another remarkable aspect is excellent solubility of Azo-POSS in the BPLC system as determined from the homogeneous optical texture without undissolved particles

and the drop of aforementioned $T_{\text{Iso-BPII}}$ and $T_{\text{BPII-N*}}$ temperatures with an increase of the photoresponsive dopant. Such solubility was satisfying even when the doping concentration exceeded 30.0 wt%, which has not been achieved in previously reported photoresponsive materials.[24] The better compatibility between Azo-POSS and BPLC host is probably related with the mesogenic azobenzene moieties, having a rod-like geometry similar to majority of LC molecules, grafted around the POSS. However, the BPII range was found to shrink gradually after reaching the maximum at the concentration of 26.0 wt%, probably due to the nonliquid crystalline characteristics of Azo-POSS (Figure S2b,c, Supporting Information). Reversible light-induced deformation and reconstruction of the BPII sc lattice was still achieved (Figure 2b I–IV), with a fast photoresponsiveness under the same stimulation conditions, having a response time shortened for at least one order of magnitude compared with the sample containing 2.0 wt% Azo-POSS due to the significant increase of such photosensitive dopant in the system. The sample exhibited a quick change of reflection color corresponding to a longer wavelength followed by the transformation to N* phase in a minute during UV irradiation, and then recovered to BPII with subsequent visible light irradiation. Such light reconstruction of BPII sc soft lattice showed a robust repeatability by alternately irradiating the sample with UV and visible light. It was found that no obvious change on both the typical texture and optical properties of two photostationary states, i.e., BPII and N*, was observed even after the sample was repeatedly driven for about 30 times. Furthermore, it is noteworthy that BPII was stable in the room temperature, while the photoinduced N* state was maintained for more than 48 h at a dark ambient. Stable sc BPII lattice exhibiting reversible

transformation to a helical superstructure triggered by light has not been realized so far to the best of our knowledge. These characteristics provide impetus for the applications of dynamic BP soft lattices in advanced photonic devices, especially the infrared optical fields such as the optical communication and biophotonics.

The micropatterns comprising two distinct well-defined regions of BPII and N* can be readily fabricated by harnessing the light-driven reversible transformation of the sc BPII lattice, thereby endowing the material with tremendous promising applications, such as stable diffractive photonic devices, and bringing

new conception and capabilities in fundamental science. Such a formidable task, realizing a stable prescribed biphasic distribution through a precise photomasking technology, has not been achieved so far, though an uncontrollable and undefined biphasic distribution, i.e., the coexistence of BPII and N* phase, is usually observed in films while cooling from the BPII. The BPLC containing 26.0 wt% Azo-POSS was confined in a 20 μm-thick cell without surface alignment treatment and firstly illuminated by the UV light with a uniform intensity of 1.0 mW cm^{-2} at room temperature (i.e., 25.0 °C) for about 10 s to deform the original BPII (**Figure 3**b-I) to N* (Figure 3b-II). The sample was
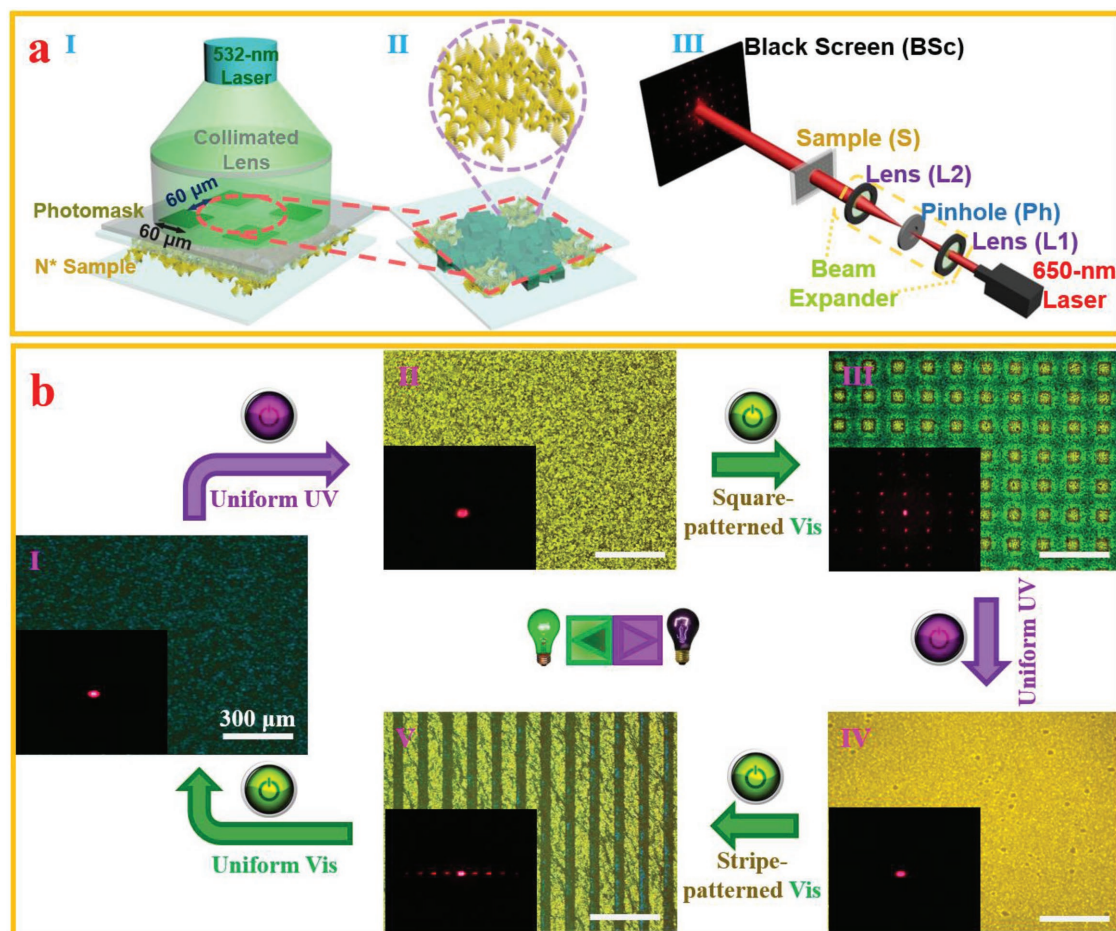

Figure 3. Dynamic and reversible light reconfiguration of biphasic micropattern formed by periodic distributed BPII and N* regions. a) The schematic pictures depicted the formation of a BPII/N* biphasic micropattern. The original BPII sample was stimulated to N* by a uniform irradiation of UV light and followed by (I) an irradiation of the collimated 532nm laser through the binary square photomask (the size of square opaque areas and the space between the adjacent opaque areas are 60 μm) for more than 25 s. (II) At the transparent areas of the photomask, N* phase recovered to BPII arrangement, while the N* phase was maintained at the opaque squares, thereby forming the periodic square N* "island" array regularly distributed in the "sea" of BPII. (III) The optical diffraction behavior of the biphasic micropattern was detected through the setup, formed by a semiconductor laser (650 nm, intensity: 0.5 mW cm^{-2}), which sequentially passed through a lens (L1, focal length: 6 cm), a pinhole (Ph, diameter: 10 μm), and another lens (L2, focal length: 15 cm) to avoid the stray light as well as expand and collimate the beam. The light impinged on the sample (S) along the cell normal; and a black screen (BSc) was settled on the backside of the sample to receive the diffraction pattern. b) Light rewritability of the biphasic micropattern by an alternate irradiation of UV (365 nm) and visible (532 nm) lights. The original (I) BPII was transited to (II) N* by an irradiation with uniform UV light for 10 s. (III) A biphasic micropattern, exhibiting periodic square N* regions distributed in the "sea" of BPII, was formed by an irradiation with a square-patterned visible light through the photomask depicted in (a-I). (IV) Such square pattern can be erased and transited back to N* phase by a following 10 s irradiation with a uniform UV light after removing the photomask. (V) A stripe biphasic micropattern can be rewritten by a stripe-patterned visible light through a binary stripe photomask (the sizes of transparent and opaque stripes are 60 μm) for 30 s. The stripe pattern can be recovered to the original BPII by removing the photomask and irradiating the sample with a uniform visible light for about 30 s. Inset of every panel in (b) showed the corresponding diffraction pattern detected with the optical setup in (a-III). Herein, the intensities of UV and visible lights were 1.0 and 10.0 mW cm^{-2}, respectively. Cell thickness was 20 μm. Scale bar in (b) was 300 μm. The experiment was performed at room temperature, i.e., 25.0 °C.

subsequently irradiated by a collimated 532 nm laser with a uniform intensity of 10.0 mW cm^{-2} through a periodic binary square photomask (the size of the opaque squares and space between the adjacent squares are 60 µm) for more than 25 s, thereby generating the square N* "islands" periodically positioned in a "sea" of BPII, displaying the optically isotropic BPII at the exposed regions while the light-scattered N* at unexposed areas (Figure 3b-III). A 650 nm semiconductor laser was generated and impinged on the sample by passing through a beam expander, composed of a pair of lens (i.e., L1 and L2) and a pinhole spatial filter (i.e., Ph), to avoid the adverse impact from stray light as well as obtain a collimated detected beam (Figure 3a-I). A clear 2D far-field diffraction array was received on a black receiving screen (Figure 3b-III), which probably resulted from the periodic modulation of transmitted light intensity due to the light transmission contrast between transparent BPII and light-scattered N* according to scalar diffraction theory, which was applied in previous works.[25] In contrast, no diffraction occurred in both pure BPII and the N* films (Figure 3b-I,II). The square micropattern can be erased by a uniform UV light irradiation (Figure 3b-IV) and rewritten to any arbitrary patterns by a following photolithography, such as the straight stripe pattern (Figure 3b-V), with 532 nm visible light. The whole system can recover to the original BPII with a subsequent irradiation with uniform 532 nm light. Furthermore, the possibility for generating a complementary biphasic micropattern, i.e., replacing the BPII and N* regions in the pattern, with a UV light exposure followed by visible light stimulation was achieved (Figure S8, Supporting Information). Such a reversible and dynamic photoresponsiveness enables all-optical writing, erasing, and rewriting with regard to a soft sc crystal and producing the elegant soft and fluid "alloy" composed by 3D BPII and 1D N*.

In conclusion, we have, for the first time, demonstrated a reversible transformation between a 3D soft sc lattice and 1D helical superstructure in a BPLC by doping a judiciously designed and synthesized photosensitive molecular switch functionalized nanocage. Distinct from the previously used photosensitive molecular switches, a stable BPII sc arrangement of LC molecules, covering room temperature, was obtained and the lattice constant was continuously tuned by light irradiation enabled by the specially designed molecular switch functionalized nanocage. A dynamic and reversible photoinduced switching between the high symmetric BPII lattice and the low symmetric 1D helical superstructure was achieved by an alternate irradiation with UV and visible lights, which has not been reported earlier to the best of our knowledge. Leveraging this capability, unprecedented light-driven recording, erasing, and rewriting of well-defined biphasic (i.e., BPII and N*) micropatterns have been demonstrated for the first time and photonic applications of such biphasic micropattern were explored. The challenging task achieved herein reveals great possibilities for applications in the fields of soft matter, crystallography, electronics, and photonics and could inspire tremendous interest for both fundamental studies and technological explorations.

Experimental Section

Materials: The photoresponsive BPLC was fabricated using the commercially available nematic LC, TEB3X (provided by Slichem Co. Ltd., China), the photoinsensitive chiral agent, R5011 (supported by HCCH, China), and the photosensitive azobenzene functionalized POSS nanocage, **Azo-POSS**, synthesized in our lab (see Supporting Information). The concentration of **Azo-POSS** was gradually increased to 34.0 wt% with a step of 2.0 wt%, while the content of chiral agent in the mixture was maintained to a constant of 3.6 wt% to maintain chirality of the whole system. The mixture was stirred at the corresponding clearing point for at least 1 h and injected into the 5 µm-thick LC cell assembled from two indium tin oxide (ITO) coated glass substrates without any surface treatment. Here we note that the cell gap was increased to 20 µm in micropattern writing, erasing, and rewriting for enhancing the photonic effect.

Measurements: The sample was settled on a precisely controlled hot stage (LTS120E, Linkam) and cooled from the clearing point at a rate of 0.2 °C min^{-1}. The phase transition behavior of the sample was observed by a polarized optical microscopy (POM, Nikon LVPOL 100) with crossed polarizers under reflection mode and the optical textures were captured by a charge-coupled device (CCD, DS-U3, Nikon) mounted on the POM. A capacitance meter (Hitester 3532–50, Hioki) was connected to the ITO substrates to detect the capacitance of the sample during the cooling process; meanwhile, the reflection spectrum of the sample was monitored by a fiber spectrometer (ULS2048, Avantes) connected to the POM. The corresponding Kössel diagram was detected by the reflection mode using a monochromatic laser source and a high numerical aperture (NA) oil immersed objective (×100/NA = 1.25, oil, Plan, Nikon); thus, the diagram was received at the back focal plane of the objective. As reported previously,[6b,7a,19] the BPII was identified in accordance with the blue-shift of the corresponding reflection spectrum during the sample cooling and in combination of the Kössel diagram. Additionally, a 365 nm UV LED source and a 532 nm yttrium aluminum garnet frequency-doubled laser were utilized as the light-stimuli to trigger the transformation of BPII sc soft lattice. The output intensity of the UV LED and the laser were adjusted to 1.0 and 10.0 mW cm^{-2}, respectively.

Supporting Information

Supporting Information is available from the Wiley Online Library or from the author.

Conflict of Interest

The authors declare no conflict of interest.

[1] a) J. J. Choi, C. R. Bealing, K. Bian, K. J. Hughes, W. Zhang, D. M. Smilgies, R. G. Hennig, J. R. Engstrom, T. Hanrath, *J. Am. Chem. Soc.* **2011**, *133*, 3131; b) Z. Quan, H. Xu, C. Wang, X. Wen,

Y. Wang, J. Zhu, R. Li, C. J. Sheehan, Z. Wang, D. M. Smilgies, Z. Luo, J. Fang, *J. Am. Chem. Soc.* **2014**, *136*, 1352.

[2] Q. Chen, S. C. Bae, S. Granick, *Nature* **2011**, *469*, 381.

[3] H. Mundoor, B. Senyuk, I. I. Smalyukh, *Science* **2016**, *352*, 69.

[4] U. Tkalec, M. Ravnik, S. Copar, S. Zumer, I. Musevic, *Science* **2011**, *333*, 62.

[5] C. Kittel, *Introduction to Solid State Physics*, John Wiley & Sons, NY **2005**.

[6] a) S. T. Hur, B. R. Lee, M. J. Gim, K. W. Park, M. H. Song, S. W. Choi, *Adv. Mater.* **2013**, *25*, 3002; b) L. Wang, Q. Li, *Adv. Funct. Mater.* **2016**, *26*, 10; c) T.-H. Lin, C.-W. Chen, Q. Li, *Anisotropic Nanomaterials: Preparation, Properties, and Applications* (Ed: Q. Li), Springer, Heidelberg **2015**, Ch. 9; d) J. B. Guo, Y. Shi, X. Han, O. Jin, J. Wei, H. Yang, *J. Mater. Chem. C* **2013**, *1*, 947.

[7] a) H. Choi, H. Higuchi, H. Kikuchi, *Appl. Phys. Lett.* **2011**, *98*, 131905; b) H. Yoshida, K. Anucha, Y. Ogawa, Y. Kawata, M. Ozaki, J. I. Fukuda, H. Kikuchi, *Phys. Rev. E* **2016**, *94*, 042703.

[8] a) X. Chen, L. Wang, C. Li, J. Xiao, H. Ding, X. Zhang, W. He, H. Yang, *Chem. Commun.* **2013**, *49*, 10097; b) O. Y. Jin, D. W. Fu, J. Wei, H. Yang, J. B. Guo, *RSC Adv.* **2014**, *4*, 28597.

[9] T. H. Lin, Y. Li, C. T. Wang, H. C. Jau, C. W. Chen, C. C. Li, H. K. Bisoyi, T. J. Bunning, Q. Li, *Adv. Mater.* **2013**, *25*, 5050.

[10] a) M. Ravnik, G. P. Alexander, J. M. Yeomans, S. Zumer, *Proc. Natl. Acad. Sci. USA* **2011**, *108*, 5188; b) M. A. Gharbi, S. Manet, J. Lhermitte, S. Brown, J. Milette, V. Toader, M. Sutton, L. Reven, *ACS Nano* **2016**, *10*, 3410.

[11] a) D.-Y. Kim, S. Kim, S.-A. Lee, Y.-E. Choi, W.-J. Yoon, S.-W. Kuo, C.-H. Hsu, M. Huang, S. H. Lee, K.-U. Jeong, *J. Phys. Chem. C* **2014**, *118*, 6300; b) W.-J. Yoon, Y.-J. Choi, D.-Y. Kim, J. S. Kim, Y.-T. Yu, H. Lee, J.-H. Lee, K.-U. Jeong, *Macromolecules* **2016**, *49*, 23.

[12] a) R. Sastre, V. Martín, L. Garrido, J. L. Chiara, B. Trastoy, O. García, A. Costela, I. García-Moreno, *Adv. Funct. Mater.* **2009**, *19*, 3307; b) S.-C. Chen, J.-D. Lin, C.-R. Lee, S.-J. Hwang, *J. Phys. D: Appl. Phys.* **2016**, *49*, 165102.

[13] P. Nayek, A. Mukherjee, H. Jeong, S. W. Kang, S. H. Lee, H. Yokoyama, *J. Nanosci. Nanotechnol.* **2013**, *13*, 4072.

[14] E. Kemiklioglu, J. Y. Hwang, L. C. Chien, *Phys. Rev. E* **2014**, *89*, 042502.

[15] H.-Y. Liu, C.-T. Wang, C.-Y. Hsu, T.-H. Lin, J.-H. Liu, *Appl. Phys. Lett.* **2010**, *96*, 121103.

[16] L. Wang, K. G. Gutierrez-Cuevas, H. K. Bisoyi, J. Xiang, G. Singh, R. S. Zola, S. Kumar, O. D. Lavrentovich, A. Urbas, Q. Li, *Chem. Commun.* **2015**, *51*, 15039.

[17] a) J. Wang, C. G. Lin, J. Y. Zhang, J. Wei, Y. F. Song, J. B. Guo, *J. Mater. Chem. C* **2015**, *3*, 4179; b) J. Wang, C. G. Lin, J. Li, J. Wei, Y. F. Song, J. B. Guo, *Mol. Cryst. Liq. Cryst.* **2016**, *634*, 12.

[18] S. Y. Jo, S. W. Jeon, B. C. Kim, J. H. Bae, F. Araoka, S. W. Choi, *ACS Appl. Mater. Interfaces* **2017**, *9*, 8941.

[19] a) H. J. Coles, M. N. Pivnenko, *Nature* **2005**, *436*, 997; b) K. W. Park, M. J. Gim, S. Kim, S. T. Hur, S. W. Choi, *ACS Appl. Mater. Interfaces* **2013**, *5*, 8025; c) K. Kim, S.-T. Hur, S. Kim, S.-Y. Jo, B. R. Lee, M. H. Song, S.-W. Choi, *J. Mater. Chem. C* **2015**, *3*, 5383.

[20] a) Z. Zheng, B. Liu, L. Zhou, W. Wang, W. Hu, D. Shen, *J. Mater. Chem. C* **2015**, *3*, 2462; b) Z. Zheng, Y. Li, H. K. Bisoyi, L. Wang, T. J. Bunning, Q. Li, *Nature* **2016**, *531*, 352.

[21] H. Kikuchi, M. Yokota, Y. Hisakado, H. Yang, T. Kajiyama, *Nat. Mater.* **2002**, *1*, 64.

[22] P. Nayek, N. H. Park, S. C. Noh, S. H. Lee, H. S. Park, H. J. Lee, C.-T. Hou, T.-H. Lin, H. Yokoyama, *Liq. Cryst.* **2015**, *42*, 1111.

[23] P. G. De Gennes, J. Prost, *The Physics of Liquid Crystals*, Oxford University Press, Oxford **1993**, Ch. 3.

[24] a) X. Tong, Y. Zhao, *Chem. Mater.* **2009**, *21*, 4047; b) Y. Wang, A. Urbas, Q. Li, *J. Am. Chem. Soc.* **2012**, *134*, 3342; c) H. K. Bisoyi, Q. Li, *Chem. Rev.* **2016**, *116*, 15089.

[25] a) Z. Zheng, C. L. Yuan, W. Hu, H. K. Bisoyi, M. J. Tang, Z. Liu, P. Sun, W. Q. Yang, X. Wang, D. Shen, Y. Li, F. F. Ye, Y. Q. Lu, G. Li, Q. Li, *Adv. Mater.* **2017**, *29*, 1703165; b) P. Sun, Z. Liu, W. Wang, L. L. Ma, D. Shen, W. Hu, Y. Q. Lu, L. Chen, Z. Zheng, *J. Mater. Chem. C* **2016**, *4*, 9325.